Journal of Neuroscience Methods 195 (2011) 185–193

Contents lists available at ScienceDirect

Journal of Neuroscience Methods

journal homepage: www.elsevier.com/locate/jneumeth

Automated analysis of neuronal morphology, synapse number and synaptic recruitment

Sabine K. Schmitz[a,1], J.J. Johannes Hjorth[b,1], Raoul M.S. Joemai[c], Rick Wijntjes[a], Susanne Eijgenraam[a], Petra de Bruijn[a], Christina Georgiou[a], Arthur P.H. de Jong[a], Arjen van Ooyen[b], Matthijs Verhage[a], L. Niels Cornelisse[a,1], Ruud F. Toonen[a,*,1], Wouter Veldkamp[c,1]

[a] Functional Genomics, Center for Neurogenomics and Cognitive Research (CNCR), VU University Amsterdam, De Boelelaan 1085, 1081 HV Amsterdam, The Netherlands
[b] Integrative Neurophysiology, Center for Neurogenomics and Cognitive Research (CNCR), VU University Amsterdam, De Boelelaan 1085, 1081 HV Amsterdam, The Netherlands
[c] Department of Radiology, Leiden University Medical Center, Albinusdreef 2, 2333 ZA Leiden, The Netherlands

ARTICLE INFO

Article history:
Received 3 November 2010
Received in revised form
30 November 2010
Accepted 1 December 2010

Keywords:
Neuronal morphology
Immuno-fluorescence
Synapses
Dendrites
Image analysis
Synaptopathies

ABSTRACT

The shape, structure and connectivity of nerve cells are important aspects of neuronal function. Genetic and epigenetic factors that alter neuronal morphology or synaptic localization of pre- and post-synaptic proteins contribute significantly to neuronal output and may underlie clinical states. To assess the impact of individual genes and disease-causing mutations on neuronal morphology, reliable methods are needed. Unfortunately, manual analysis of immuno-fluorescence images of neurons to quantify neuronal shape and synapse number, size and distribution is labor-intensive, time-consuming and subject to human bias and error.

We have developed an automated image analysis routine using steerable filters and deconvolutions to automatically analyze dendrite and synapse characteristics in immuno-fluorescence images. Our approach reports dendrite morphology, synapse size and number but also synaptic vesicle density and synaptic accumulation of proteins as a function of distance from the soma as consistent as expert observers while reducing analysis time considerably. In addition, the routine can be used to detect and quantify a wide range of neuronal organelles and is capable of batch analysis of a large number of images enabling high-throughput analysis.

1. Introduction

Cognitive function relies on proper wiring and functional connections within neuronal circuits. Many brain disorders ranging from mental retardation and neurodegeneration, to psychiatric disorders (reviewed in Lin and Koleske (2010)) have defects in neuronal morphology. Genetic mouse models and *in vitro* studies are widely used to investigate the molecular mechanisms of these brain disorders (Groffen et al., 2010; Jockusch et al., 2007; Kawabe et al., 2010; Priller et al., 2007). Thorough and consistent quantification of different aspects of neuronal morphology is vital to gain insight in the underlying pathogenic pathways.

Manual quantification of neuronal morphology is very labor-intense, especially when measurements of multiple aspects of morphology (ranging from soma and dendrite morphology, synapse number and localization to synaptic recruitment of proteins of interest) are desired. However, most available programs focus on automation of single parameter analysis such as (semi)-automated neurite tracing in 2D and 3D preparations (Losavio et al., 2008; Meijering, 2010; Meijering et al., 2004; Narro et al., 2007; Scorcioni et al., 2008; Yu et al., 2009). To our knowledge, no software is available to automatically detect synaptic regions and report synapse intensity and synaptic recruitment of proteins of interest. Therefore, for analysis of these parameters, regions of interest need to be placed around synapses and in the soma manually by the observer.

In addition to being time-consuming, manual analysis of neuronal morphology is prone to observer bias. Not only lack of consistency within an individual observer, but also variance between different observers can reduce the level of reproducibility.

To overcome these problems, we have developed a synapse and neurite detection program called SynD (**Syn**apse **D**etector) for automated analysis of neuronal morphology. SynD has an intuitive user interface and can therefore easily be used by scientists without prior image processing experience. The program auto-

* Corresponding author. Tel.: +31 20 5986946; fax: +31 20 5986926.
E-mail address: ruud.toonen@cncr.vu.nl (R.F. Toonen).
[1] These authors equally contributed to the work.

0165-0270/$ – see front matter © 2010 Elsevier B.V. All rights reserved.
doi:10.1016/j.jneumeth.2010.12.011

matically detects the soma, dendrites (using steerable filters) and synapses (using deconvolution and thresholding) and quantifies a wide spectrum of neuronal morphology measures simultaneously. In addition to classical parameters such as dendrite length and synapse number, it measures dendritic branching using Sholl analysis, reports the localization of synapses, synapse area and soma size. Finally, SynD quantifies synaptic fluorescence intensity in up to 3 channels in the soma and synapses and calculates their ratios and cumulative probability. We tested SynD by comparing to three human observers and show that it operates at the level of expert observers and demonstrate its use to detect synaptic levels of proteins of interest.

Importantly, SynD also accurately reports the number, size, localization and density of other cellular organelles such as lysomes, endosomes and secretory vesicles and can be used on cultured neurons and fixed and living brain slices. SynD can be freely downloaded from www.cncr.nl/resources or from software.incf.org/software/synd.

2. Materials and methods

2.1. Neuronal cell culture

Isolated hippocampal neurons were plated on astrocyte microislands (Bekkers and Stevens, 1991). Astrocytes and hippocampal neurons from either wild-type or *munc18-1* heterozygous null mutant mice were prepared as described previously (de Wit et al., 2009; Toonen et al., 2006; Wierda et al., 2007). High density neuronal cultures were prepared according to de Wit et al. (2009).

2.2. Immunocytochemistry and image acquisition

Neurons were fixed in 4% paraformaldehyde at 14 days *in vitro*. Cells were labeled with antibodies against MAP2 (chicken polyclonal, 1:20000, Abcam, Cat. No. ab5392), VAMP2 (mouse monoclonal, 1:2000, SySy, Cat. No. 104 211), LAMP1 (mouse monoclonal, 1:100, Stressgen, Cat. No. Ly1C6), transferrin receptor (TfR) (mouse monoclonal, 1:500, Zymed, Cat. No. 136800), PSD-95 (mouse monoclonal, 1:250, Abcam, Cat. No. AB2723) or Munc18 (rabbit polyclonal, 1:500, SySy, Cat. No. 116 002) as described previously (Wierda et al., 2007). Secondary antibodies were Alexa488, 564 and 647-coupled anti-chicken, rabbit or mouse antibodies (1:1000, Invitrogen). Overexpression of neuropeptide (NPY)-Venus was used to label secretory vesicles. All images were captured on a laser confocal system (LSM510 meta, Carl Zeiss) with a 40× oil objective (NA 1.3) at 0.7 zoom using LSM software release version 4.2 SP1 (license basic software R 3.0).

For Fig. 6I, a layer 2/3 pyramidal neuron from a 300 μm slice of the barrel region of the somatosensory cortex of an 8 week old mouse was filled with biocytin (0.2%) using an intracellular patch-clamp recording pipette. The slice preparation was fixed in paraformaldhyde in PBS and then processed for staining with the chromogen 3,3′diaminobenzidine tetrahydrochloride (DAB) using the avidin–biotin–peroxidase method (Horikawa and Armstrong, 1988). For Fig. 6K, a layer 2/3 pyramidal neuron from a 300 μm medial prefrontal cortex coronal brain slice of a P14 mouse was filled with Alexa 594 (40 μM, Molecular Probes) via an intracellular patch pipette. The dye was allowed to diffuse for 20 min before the pipette was withdrawn, causing the somatic membrane to reseal. The neuron was then imaged using a LEICA RS2 two-photon laser scanning microscope with a 63× objective and Ti:Sapphire laser tuned to 840 nm excitation. *Z*-stacks were taken using 1 μm *Z* step intervals of overlapping regions of the neuron. These images were then stitched together and *Z*-compressed using Image J (NIH) software.

2.3. Image processing

SynD utilizes the MATLAB platform version 2009a (or later) requiring the statistics and imaging toolboxes. The program also runs as a stand-alone version in Windows and MacOS. Detection and analysis is divided into five steps (Fig. 1B). In the first step the user selects an RGB image to load and specifies the channels and resolution. The second step is soma detection. The third step is automatic neurite detection with the option to edit the neurite mask. This is followed by synapse detection as the fourth step. The fifth and final step is analysis and exporting the data as XML file to Microsoft Excel (Microsoft, Redmond, WA, USA) or OpenOffice.

Step 1: Loading the image

The user selects an RGB TIFF or LSM file to load, and then specifies which channels contain morphology information, synapse staining and the staining of a protein of interest, and in which colors they should be represented. The image resolution is read from the LSM file or, when importing TIFF files, the user can specify pixel size manually.

Step 2: Soma detection

First the image is low-pass filtered using a 2D adaptive Wiener filter (Lim, 1990) to reduce noise levels (Supplementary Fig. 1A and B). The function filters the image adaptively, using neighborhoods of 7×7 pixels and assuming the noise is Gaussian distributed. The image is then thresholded to separate image background and foreground (Supplementary Fig. 1C). The soma is separated from connected neurites by performing a morphological opening (erosion followed by dilation) using a disk with radius 15 pixels as the structural element (Supplementary Fig. 1D and E). The program then randomly places ten non-overlapping circular regions of interest in the soma to quantify protein expression. If needed, the user can select regions of the image (for example bright regions due to air bubbles in the mounting medium) to be excluded from the analysis in this step.

Step 3: Neurite detection

Neurites appear as bright ridges surrounded by dark regions. Starting from the soma the neurites are traced using local criteria. To identify which pixels are part of the neurite structure a steerable filter is applied to the image (Meijering et al., 2004) (Supplementary Fig. 2A). The filter is based on higher order derivatives of Gaussians G and is applied to the image f.

$$f_{ij} = -(f * G_{ij})$$
$$G_{ij} = \frac{\partial^2 G}{\partial_i \partial_j} \quad (1)$$

where * denotes the spatial convolution, and the indexes i, j can be in the directions x or y. The optimal direction of the steerable filter and the similarity to a neurite is calculated from the eigenvalues and eigenvectors of the Hessian matrix H.

$$H_f(x) = \begin{bmatrix} f_{xx} & f_{xy} \\ f_{yx} & f_{yy} \end{bmatrix} \quad \text{where} f_{xy} = f_{yx} \quad (2)$$

To determine whether a pixel should be added to a neurite by the neurite tracing algorithm we use a cost function previously defined in Meijering et al. (2004).

$$C(p, q) = \gamma C_\lambda(q) + (1 - \gamma) C_v(p, q) \quad (3)$$

where $\gamma \in [0,1]$ determines the relative contributions of the two cost components. The first part of the cost function (C_λ) indicates how similar the surrounding of the new pixel is to a ridge, the second part of the cost function (C_v) indicates how similar the direction from the old to the new pixel is with the directions of

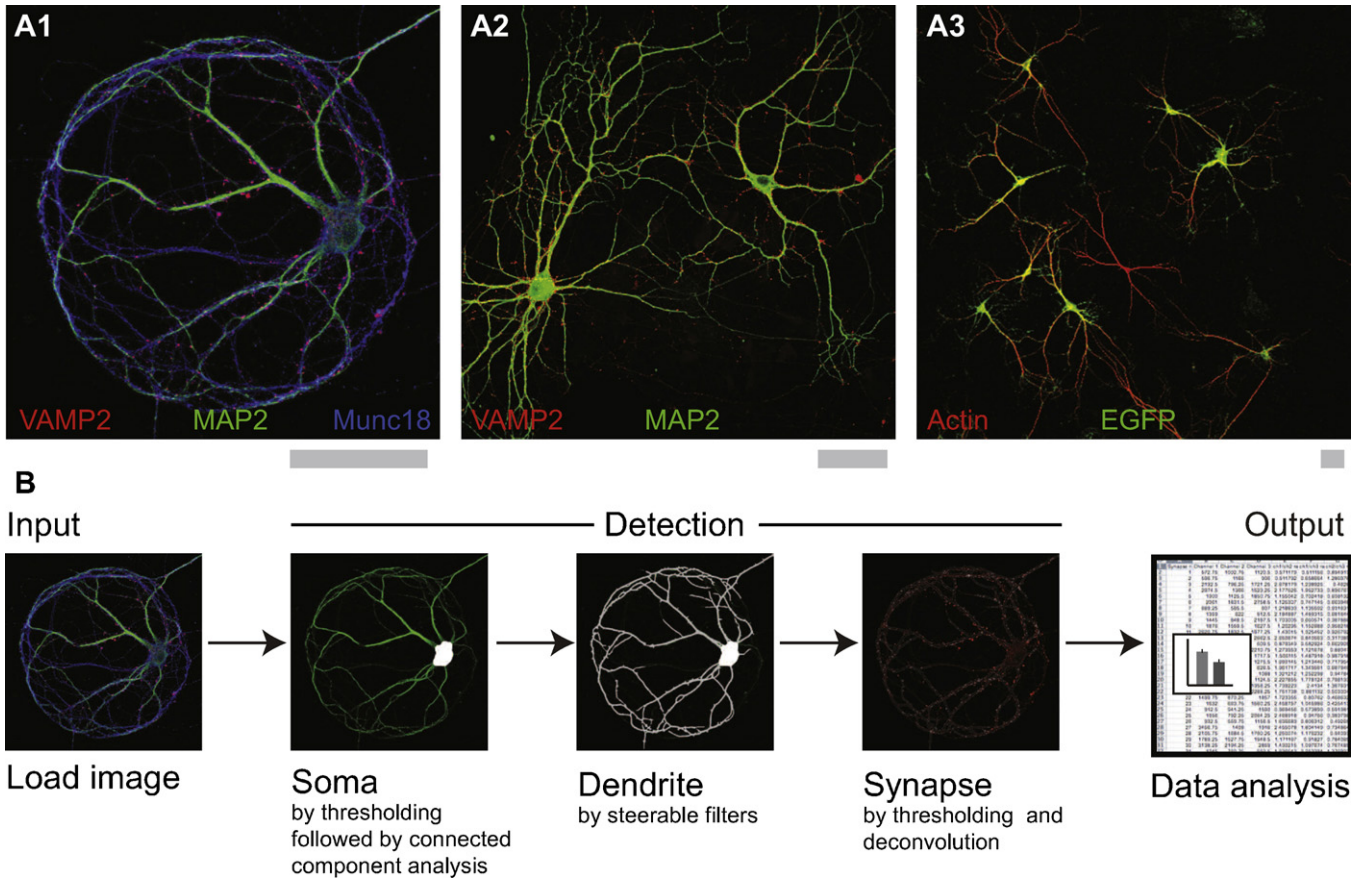

Fig. 1. Schematic representation of the 5 steps of neuronal morphology analysis by SynD. (A) Representative pictures of neuronal culture types that can be analyzed with SynD: single neuron micro-island cultures (A1), single filled or transfected neuron within a neuronal network (A2) and neuronal population (A3). Grey scale bars represent 50 μm. (B) Schematic representation of the 5 steps of neuronal morphology analysis by SynD. Pictures show a neuron stained for MAP2 (green) as dendritic marker, VAMP2 (red) as synaptic marker and Munc18 (blue) as protein of interest, which mostly localizes into axons.

the ridge around the new pixel (Supplementary Fig. 2B). Here

$$C_\lambda(q) = 1 - \rho(q)$$

$$\rho(q) = \begin{cases} \lambda(q)/\lambda_{\max} & \lambda > 0 \\ 0 & \lambda \leq 0 \end{cases} \quad (4)$$

where $\lambda_{\max}$ denotes the largest eigenvalue (λ) in the image.

$$C_v(p,q) = \tfrac{1}{2}\left(\sqrt{1-\varphi(p,q)} + \sqrt{1-\varphi(p,q)}\right) \quad (5)$$

with p and q two points in the image, and

$$\varphi(p,q) = \left|w(p)\cdot d(p,q)\right|$$

where $w(p)$ is the normalized eigenvector at p and $d(p,q) = (q-p)/\|q-p\|$ is the normalized direction vector between the points p and q. The algorithm starts with a seed point, and then calculates the cost of all pixels surrounding the seed point using Eq. (3). Pixels below the cost threshold are added to the neurite. This procedure is continued until there are no more pixels below the cost threshold to add (Supplementary Fig. 2C). A second pass of the steerable filter detection using smaller filter kernel allows detection of thinner neurites. Our approach differs from the tracing in Meijering et al. (2004) where two manually selected points are connected by the most likely path (as defined by the lowest cost), whereas we start from the soma and detect all connecting neurites by adding new pixels as long as the cost is lower than a threshold (here 0.9 was high enough to allow inclusion of most neurites without adding spurious regions to the detected neurite tree).

The intensity of the neurite staining might vary, with parts of a neurite being weakly stained, leading to partial detection of neurites. To address this problem, SynD automatically reconnects orphaned branches: from the neurites' end points the algorithm takes a small step of 5 μm outward to try and bypass weaker stained parts of the neurite scanning a region within ±15° of the neurite axis to search for potential neurites as defined by the cost function. Detected neurites are automatically connected to the rest of the neuron. The user can inspect the final neurite tree and make corrections if necessary. The program shows unconnected branches in a darker color than those connected to the soma, allowing for easy identification of orphaned branches.

Step 4: Synapse detection

Synapses appear as bright regions in the synapse channel. The algorithm first identifies putative synapse pixels by thresholding the image, requiring putative synapses to be one standard deviation above the mean synapse channel intensity. As synapses are formed on the postsynaptic dendrites, putative synapse pixels more than 1 μm from a neurite are excluded. Also regions smaller than 0.35 μm^2 are considered to be noise and discarded. In order to identify individual synapses it is necessary to separate synapses with overlapping pixels in synapse clusters. Therefore, the program looks for synapse regions with unique local intensity maxima. These single-synapse regions are then averaged together to generate a typical single synapse kernel. To identify individual synapses in synapse clusters, the image is deconvolved with the single synapse kernel. For synapse clusters that contain multiple centers, each synapse pixel is assigned to the closest center to

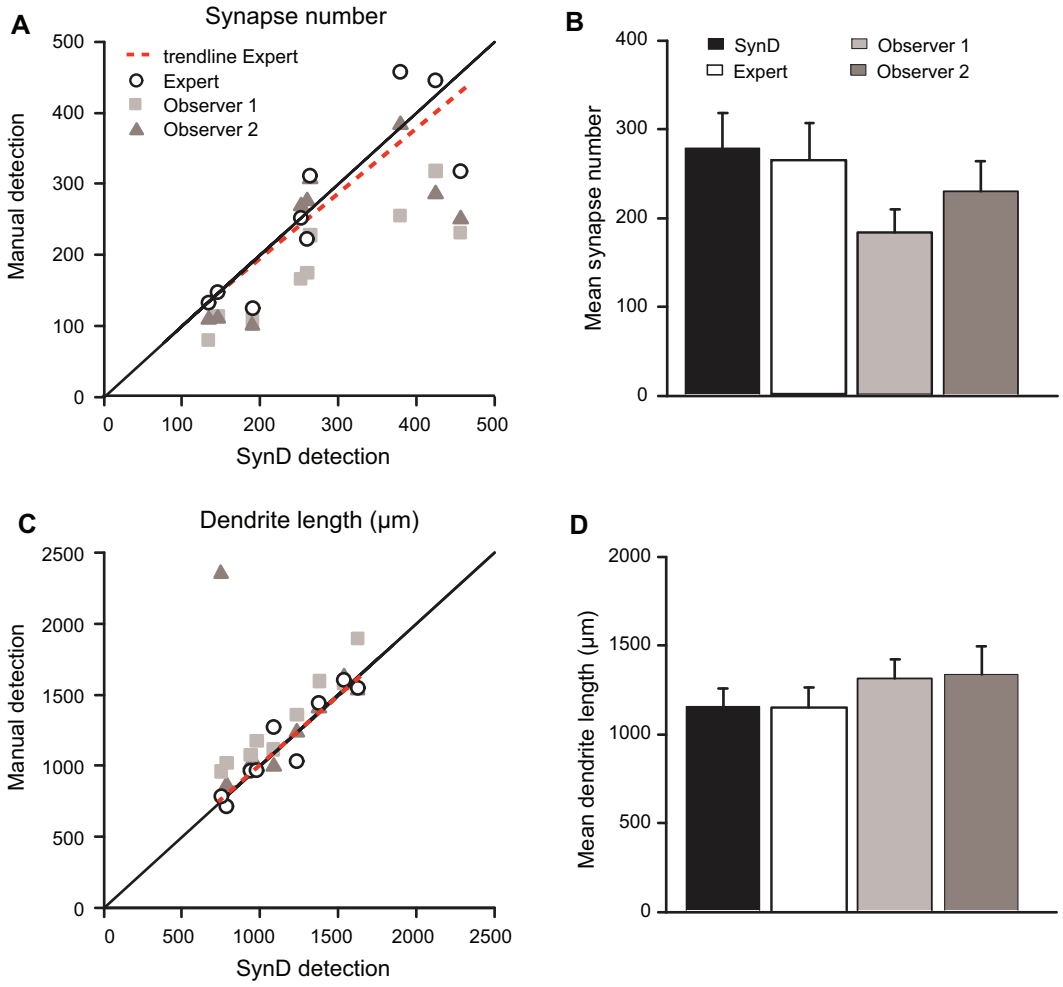

Fig. 2. Evaluation of synapse- and dendrite-detection by SynD. Data generated by SynD on synapse number (A and B) and dendrite length (C and D) is compared to manual quantification by one expert and two novice observers. (A and C) Scatter plots of individual cells ($n = 9$). Black diagonal line indicates perfect correlation. Dotted trend lines indicate predicted Y values for the expert observer. (B and D) mean values. Error bars represent S.E.M.

calculate average intensity and synapse size. Optionally, the user can specify the kernel as a two-dimensional Gaussian with a given width in order to identify structures of other sizes, like endosomes, mitochondria or secretory vesicles.

Step 5: Data analysis

To calculate dendrite length, the dendrite mask is skeletonized using MATLAB's built in bwmorph function to obtain a single-pixel representation. The distances between the centers of neighboring pixels in the dendrite skeleton are summed together to obtain dendrite length. Synapse number is defined as the number of synaptic centers found by deconvolving the synapse channel using the synapse kernel (see synapse detection). The number of synapses per unit of dendrite length is calculated by dividing the total number of detected synapses by the total dendrite length. Synapse size is defined as the number of pixels within the detected synapse region surrounding the synapse center. If there is more than one center in a synapse region, the pixels are assigned to the closest synapse center. Synapse size is converted from pixels to surface area in μm^2 when exporting the data to XML output files. To quantify dendritic branching, concentric circles are placed with increasing radius around the soma (increments of 5 μm). The program calculates the number of dendrite crossings per ring, also known as Sholl analysis (Sholl, 1953). The first circle starts at a distance equal to the maximum radius of the soma.

SynD reports the coordinates of the centers of each individual synapse. Additionally, a histogram is created reporting the number of synapses between two subsequent circles of the Sholl analysis. SynD measures the fluorescence intensity of all channels within the detected synapses. Per channel, the program reports the average intensity of the individual synapses, a normal and cumulative histogram and the average intensity. The program also calculates the intensity ratio, comparing all three channels in every synapse. For soma morphology measures, SynD reports soma area, length of the minor and major soma axis and the ratio thereof as well as soma intensity in ten regions of interest. Furthermore SynD calculates synaptic recruitment as the ratio between synaptic and somatic intensity.

2.4. Method evaluation

One expert and two novice observers quantified confocal images manually. Novice observers were familiar with imaging data and were given instructions by the expert observer (>5 years experience in fluorescent image analysis). Manual image analysis was done in ImageJ 1.43j (Abramoff, 2004). Semi-manual tracing and quantification of dendrites was performed with the plugin NeuronJ 1.4.0 (Meijering et al., 2004). NeuronJ provides semi-automated neurite tracing and is thereby already more time-efficient and precise compared to fully manual tracing. For synapse count and synapse intensity measurements, regions of interest of fixed size were manually placed around VAMP2 accumulations. Data on den-

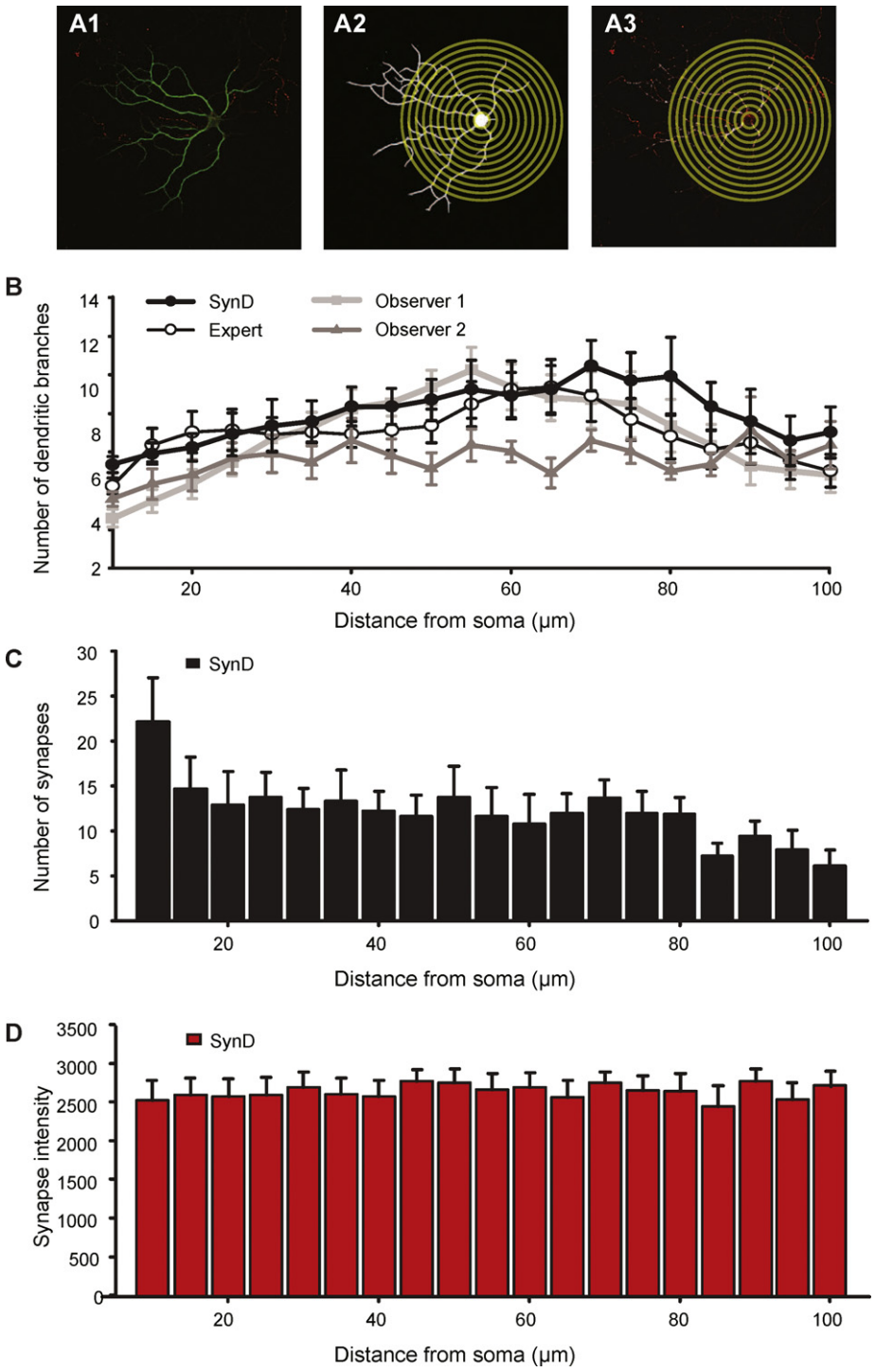

Fig. 3. Quantification of dendritic branching analysis by SynD. Example pictures of dendritic and synaptic staining (A1), dendritic mask generated by SynD (A2) with circular mask for Sholl analysis and synaptic mask generated by SynD with circular mask for synapse localization analysis (C). Distance between representative circles is 20 µm. (B) Mean number of dendritic branches plotted against distance from the soma. (C) Mean number of synapses plotted against distance from the soma. (D) Mean intensity of synapses plotted against distance from the soma. Error bars represent S.E.M.

drite length, synapse number and intensity was exported as XML file to Microsoft Excel (Microsoft, Redmond, WA, USA) and further analyzed by the expert user.

3. Results

To automatically analyze neuronal morphology, we have developed the MATLAB based program SynD (Fig. 1). SynD processes fluorescent images of neurons that are stained with antibodies against a dendritic marker (e.g. MAP2), a synaptic marker (e.g. VAMP2) and, if desired, a third protein of interest, to calculate several features of neuronal morphology. First, SynD selects the cell body, generates a dendritic mask and marks detected synaptic puncta on the dendritic mask as synapses. During this process, user interaction is possible in order to review detection and to add or delete erroneous detected objects. Finally, SynD analyzes and exports multiple morphological characteristics such as dendrite length and branching as well as synapse number, area, localization and density.

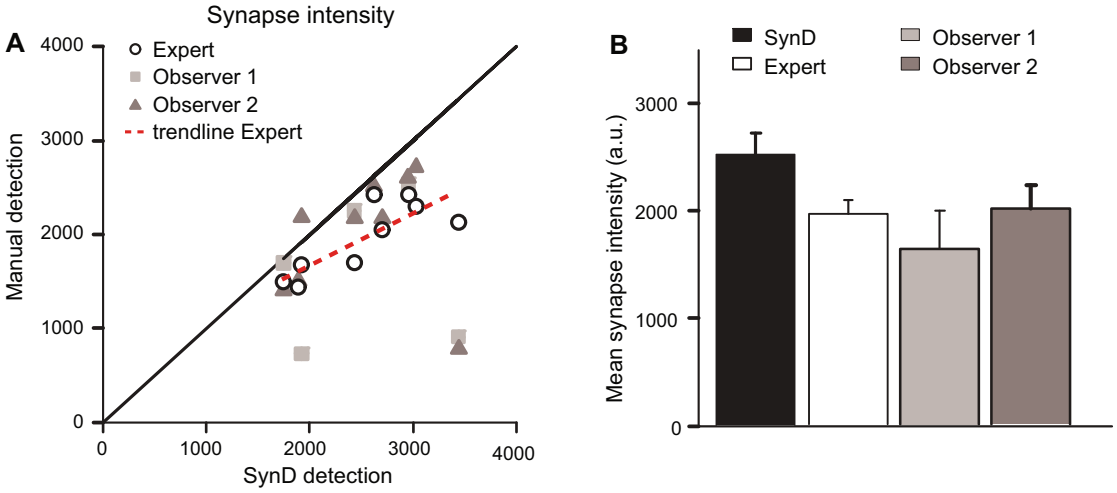

Fig. 4. Evaluation of synapse-intensity by SynD. (A and B) Data generated by the SynD is compared to manual quantification by one expert and two novice observers (Observer 1 and 2). Synapses in wild-type neurons were labeled with the synaptic vesicle marker VAMP2 and synapse intensity measured by manually placing region of interest. SynD operated at the level of the expert observer. ($N = 9$, one-way ANOVA $F(3, 28) = 2.502$, $p > 0.05$).

3.1. SynD reliably analyzes dendrite length and synapse number

To test the accuracy of SynD, we compared the results from the program with those obtained from manual analysis by an experienced observer (from here on called "expert"). Results for mean total dendrite length (one-way ANOVA, $F(3,32) = 0.5292$, $p > 0.05$) and synapse number (one-way ANOVA, $F(3,32) = 2.040$, $p > 0.05$) are similar between expert and SynD (Fig. 2A–D). This shows that SynD can be used to reliably measure dendrite length and synapse number of cultured neurons. In addition to the expert, we also asked two in-experienced users (from here on called "Observer 1 and 2") to manually quantify dendrite length and synapse number. Although on average not significantly different from the expert and SynD, measurements by novice observers deviate much more from the expert's quantification and show considerable variation between observers (Fig. 2). Hence, SynD provides a tool to minimize inter-observer bias and to bring inexperienced observers to an expert level.

3.2. SynD automatically quantifies dendritic branching and synaptic localization

Measuring dendrite length only gives a limited view of the overall morphology of a neuron. To get a more meaningful measure of neuronal morphology, one can examine the degree of dendritic branching by performing a Sholl analysis (Sholl, 1953). Starting from the soma, SynD draws circles with increasing radius (Fig. 3A). The observer can define the number of circles and distance between subsequent circles. Next, the algorithm counts the crossings of dendrites with the circles as an indicator of dendritic branching (Fig. 3B). We tested the accuracy of SynD by comparing with the results from manual observers. Again, the program functioned at the level of the experienced observer. Dendrites crossing the first radius line are considered to be primary dendrites. Additionally, the program reports the number of synapses and their intensity within each circle of the Sholl analysis as a measure of synaptic localization (Fig. 3C and D).

3.3. SynD measures synapse intensity and synaptic localization of proteins

SynD also quantifies the fluorescence intensity in detected synapses. We compared the results from SynD to manual synapse detection in ImageJ (Fig. 4). Mean synaptic intensity of individual cells was slightly lower in manual detection (one-way ANOVA $F(3, 28) = 2.502$, $p > 0.05$), most likely due to the fact that regions of interest (ROI) in manual detection contained a small number of non-synaptic pixels when using squared ROIs (Fig. 4A and B).

Furthermore, SynD quantifies the intensity of additional fluorescent channels in detected synapses. This way, one can stain for additional proteins of interest and quantify their synaptic expression levels and localization in a very efficient manner. Per channel, SynD reports the average intensity within the individual synapses, a normal and cumulative histogram and the average (±S.E.M.) intensity.

Supplementary Fig. 4 shows an example of such an application. Neurons of wild-type (WT) and *munc18-1* heterozygous null mutant (±) mice were stained for MAP2, VAMP2 and Munc18-1. Quantification of Munc18-1 expression levels in synapses showed a significant reduction in *munc18-1* heterozygous neurons (one-tailed Student's *t*-test, $p = 0.0254$), similar to reported reduced levels in total brain lysate (Verhage et al., 2000), whereas VAMP2 levels are not significantly different (Supplementary Fig. 4B and C) (two-tailed Student's *t*-test, $p > 0.05$).

In addition, SynD reports the ratio between two channels per individual ROI and group mean. This showed that the

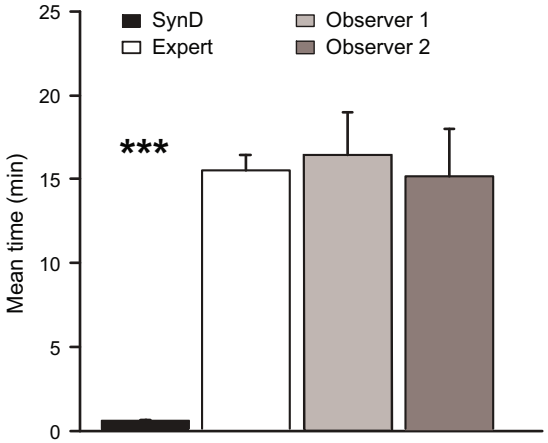

Fig. 5. Efficiency evaluation for SynD. Mean values of time needed for morphology analysis per cell. SynD reduces analysis time by more than 90%. Error bars represent S.E.M.

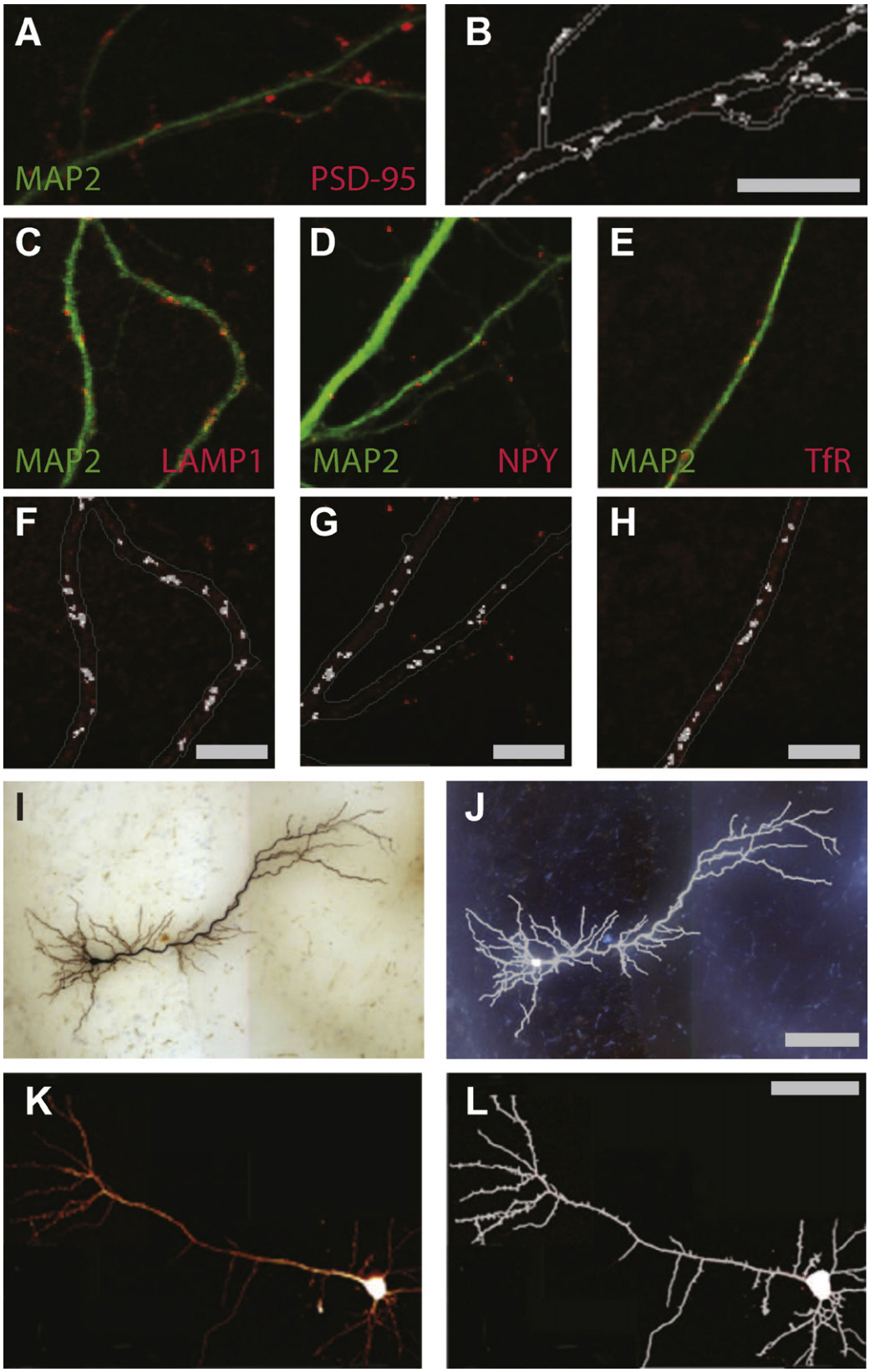

Fig. 6. SynD can also be used to analyze postsynaptic densities, cellular organelles and slice preparations. Representative pictures of hippocampal neurons stained against MAP2 for dendrite morphology and PSD-95 as postsynaptic marker (A and B), LAMP1 as lysosomal marker (C, F), neuropeptide Y (NPY) as secretory vesicle marker (D, G) or transferrin receptor (TfR) (E, H). Scale bar represents 10 μm. (A, C–E) show original images, (B) shows the "postsynapse" mask and (F–H) represent "organelle" masks as detected by SynD. (I) Representative stitched picture of a biocytin-filled, fixed neuron in a brain slice of the barrel region of the somatosensory cortex. (J) Inverted picture of (I) including the soma and neurite mask as detected by SynD. The picture shows that even in stitched images with varying signal to noise ratio, neurite detection works reliably. (K) Representative picture of a 2 photon live cell reconstruction of a layer 2/3 pyramidal neuron filled with Alexa 594 via the patch pipette. Scale bars on original individual images have been removed for clarity. (L) Neurite mask of (K) as detected by SynD.

Munc18/VAMP ratio is reduced by 41% in *munc18* heterozygous neurons (Supplementary Fig. 4D) (unpaired *t*-test with Welsh correction, $p = 0.0109$). Finally, SynD calculates the fluorescent intensity in the cell soma by randomly placing 10 ROIs in the soma. Munc18 somatic levels in *munc18* heterozygote null mutant neurons are reduced by 48% compared to wild-type (Supplementary Fig. 4E, unpaired *t*-test with Welsh correction, $p = 0.0039$). The ratio of synaptic expression and somatic expression reports the synaptic recruitment of Munc18 in wild-type and null mutant neurons (Supplementary Fig. 4F, two-tailed Student's *t*-test, $p > 0.05$).

3.4. SynD is time-efficient

To evaluate the efficiency of SynD, we measured the time needed to analyze neuronal morphology automatically or manually. Fig. 5 shows that both expert and novices need on average more than 15 min for manual analysis of a single neuron. Strikingly, SynD can do the same quantification in less than a minute on a modern desktop computer, saving more than 90% analysis time (one-way ANOVA, $F(3,32) = 14.956$, $p < 0.0001$). Importantly, the program can also operate in batch mode: once the first neuron has been analyzed the operator can select an image folder, SynD will analyze all images in this folder with the selected settings. Thus, the program allows reliable and time-efficient analysis of neuronal morphology and has the capacity to perform this analysis on a large number of images without the need for human intervention.

3.5. SynD is not limited to synapse detection in cultured neurons

In addition to single neuron micro-island cultures, SynD can also quantify neuronal morphology of individual neurons grown in a network (examples in Fig. 1A2 and A3). In addition to presynaptic markers such as VAMP2 or synapsin, SynD also allows analysis of postsynaptic densities (Fig. 6A and B). Supplementary Fig. 5 shows a representative image in which dendrites were stained with an antibody against MAP2 and postsynaptic densities were quantified as PSD-95 positive puncta on the dendrites. Furthermore, besides quantification of pre- and post-synaptic terminals, SynD can also be used to quantify the number of intra-cellular organelles in neurites. Fig. 6C–H shows examples where SynD is used to count the number of lysosomes, secretory vesicles and transferrin receptor accumulations in cultured neurons. Here, dendrites were stained for MAP2 and only organelles in the dendrite were identified. If desired, organelles can also be detected in axons when using an axonal marker or, when a space filling protein like EGFP is used, the program reports the total amount of organelles. In addition, SynD can also be used to analyze the morphology of biocytin-filled neurons in brain slices (Fig. 6I and J) or the morphology of living neurons filled with Alexa 594 in brain slices imaged with 2-photon microscopy (Fig. 6K and L).

4. Discussion

Reliable and comprehensive analysis of neuronal morphology together with quantitative measurements on synaptic protein localization and levels is an important first step in the analysis of disease-causing mutations or other genetic perturbations in synaptic proteins. Unfortunately, most of the available software is not able to provide a comprehensive analysis of all aspects of neuronal morphology, while manual analysis of neuronal morphology is labor-intensive and prone to observer-bias.

To overcome these shortcomings, we developed an image analysis routine for automated analysis of neuronal morphology. SynD is unbiased, reliable and accurate and performs at the level of an expert observer. In addition, the program is highly automated and can operate on multiple images without human intervention. This enables simultaneous analysis of multiple morphological features and high throughput screening of different genetic and pharmacological treatments. Although SynD is highly automated, user interaction is possible during all detection steps allowing optimal control for the scientist, even without any programming or image processing experience. SynD minimizes inter-observer bias and brings inexperienced observers to an expert level.

The program integrates two important novel features that will aid in the analysis of genetic perturbations that may have an impact upon synapse development or synaptic recruitment of proteins of interest. First, SynD provides information on the localization of detected synapses by reporting the number of detected synapses as a function of distance from the soma (Fig. 3C). This distinguishes between effects on proximal synapses and more distal synapses as for instance in the case of acute overexpression of the polo-like kinase 2 protein (Pak and Sheng, 2003). Second, SynD measures the expression level of proteins of interest in these detected synapses and compares the synaptic levels with the level in the cell soma (Fig. 3D and Supplementary Fig. 4E and F). This generates information on protein transport and synaptic recruitment as a function of distance traveled from the soma. In this way, it will be feasible to test the effect of genetically perturbing for instance a presynaptic scaffolding protein on the recruitment of a large number of proteins of interest.

Finally, SynD is not restricted to synapse measurements but can be applied to report on a wide variety of cellular features ranging from synapse to organelle analysis and can be used for different types of cell cultures and brain slices (Fig. 6).

Taken together, SynD is a powerful tool for automated and standardized analysis of neuronal morphology.

Acknowledgements

The authors would like to thank Dr. Rhiannon Meredith for providing images of brain slices, Dr. Tatiana Boiko for providing images of neuronal networks, Juliane Lauks for providing images of different organelle markers and Desiree Schut for testing earlier versions of the software. This work was supported by a Neuromics Marie Curie Early stage Training grant (MEST-CT-2005-020919; SKS). SKS is a recipient of the Netherlands Scientific Organization Toptalent grant (NWO 021.001.076) and JH is supported by NWO grant 635.100.017.

Appendix A. Supplementary data

Supplementary data associated with this article can be found, in the online version, at doi:10.1016/j.jneumeth.2010.12.011.

References

Abramoff MD. Image processing with imageJ. In: Magelhaes PJ, editor. Biophotonics international; 2004.

Bekkers J, Stevens C. Excitatory and inhibitory autaptic currents in isolated hippocampal neurons maintained in cell culture. Proc Natl Acad Sci USA 1991;88:7834–8.

de Wit J, Toonen RF, Verhage M. Matrix-dependent local retention of secretory vesicle cargo in cortical neurons. J Neurosci 2009;29:23–37.

Groffen A, Martens S, Díez Arazola R, Cornelisse L, Lozovaya N, de Jong A, et al. Doc2b is a high-affinity Ca^{2+} sensor for spontaneous neurotransmitter release. Science 2010;327:1614–8.

Horikawa K, Armstrong W. A versatile means of intracellular labeling: injection of biocytin and its detection with avidin conjugates. J Neurosci Methods 1988;25:1–11.

Jockusch W, Speidel D, Sigler A, Sørensen J, Varoqueaux F, Rhee J, et al. CAPS-1 and CAPS-2 are essential synaptic vesicle priming proteins. Cell 2007;131:796–808.

Kawabe H, Neeb A, Dimova K, Young SJ, Takeda M, Katsurabayashi S, et al. Regulation of Rap2A by the ubiquitin ligase Nedd4-1 controls neurite development. Neuron 2010;65:358–72.
Lim JS. Two-dimensional signal and image processing. Englewood Cliffs, NJ: Prentice Hall; 1990. p. 548.
Lin Y, Koleske A. Mechanisms of synapse and dendrite maintenance and their disruption in psychiatric and neurodegenerative disorders. Annu Rev Neurosci 2010;33:349–78.
Losavio B, Liang Y, Santamaría-Pang A, Kakadiaris I, Colbert C, Saggau P. Live neuron morphology automatically reconstructed from multiphoton and confocal imaging data. J Neurophysiol 2008;100:2422–9.
Meijering E. Neuron tracing in perspective. Cytometry A 2010;77:693–704.
Meijering E, Jacob M, Sarria J, Steiner P, Hirling H, Unser M. Design and validation of a tool for neurite tracing and analysis in fluorescence microscopy images. Cytometry A 2004;58:167–76.
Narro M, Yang F, Kraft R, Wenk C, Efrat A, Restifo L. NeuronMetrics: software for semi-automated processing of cultured neuron images. Brain Res 2007;1138:57–75.
Pak D, Sheng M. Targeted protein degradation and synapse remodeling by an inducible protein kinase. Science 2003;302:1368–73.
Priller C, Dewachter I, Vassallo N, Paluch S, Pace C, Kretzschmar H, et al. Mutant presenilin 1 alters synaptic transmission in cultured hippocampal neurons. J Biol Chem 2007;282:1119–27.
Scorcioni R, Polavaram S, Ascoli G. L-Measure: a web-accessible tool for the analysis, comparison and search of digital reconstructions of neuronal morphologies. Nat Protoc 2008;3:866–76.
Sholl D. Dendritic organization in the neurons of the visual and motor cortices of the cat. J Anat 1953;87:387–406.
Toonen RFG, Wierda K, Sons MS, de Wit H, Cornelisse LN, Brussaard A, et al. Munc18-1 expression levels control synapse recovery by regulating readily releasable pool size. Proc Natl Acad Sci USA 2006;103:18332–7.
Verhage M, Maia AS, Plomp JJ, Brussaard AB, Heeroma JH, Vermeer H, et al. Synaptic assembly of the brain in the absence of neurotransmitter secretion. Science 2000;287:864–9.
Wierda KDB, Toonen RFG, de Wit H, Brussaard AB, Verhage M. Interdependence of PKC-dependent and PKC-independent pathways for presynaptic plasticity. Neuron 2007;54:275–90.
Yu W, Lee H, Hariharan S, Bu W, Ahmed S. Quantitative neurite outgrowth measurement based on image segmentation with topological dependence. Cytometry A 2009;75:289–97.